

PRECIPITATION AND ANNEALING-OUT OF LATTICE DEFECTS  
IN SPLAT-COOLED Al-Fe ALLOYSEberhard Blank, Institut für Werkstoffe  
Ruhr-Universität Bochum  
Germany

By piston and anvil technique Al-alloys containing 0.05 up to 2 at-% Fe have been quenched from the melt. The melts were superheated to about 400 degrees above the liquidus temperature. On one hand differences in the cooling rate lead to a phase separation with dendritic crystallisation, while on the other hand supersaturated solid solutions are obtained.

The distribution and density of defects quenched in is strongly related to the process of solidification. During dendritic crystallisation, defects are used to form phase boundaries between matrix and precipitates as well as to build subgrain boundaries. The matrix is depleted from precipitates and defects. In supersaturated solid solutions the dislocation density increases with the concentration of iron while the density of vacancy dislocation loops decreases with increasing concentration.

The micro-hardness of the as-quenched solid solutions increases more rapidly with concentration than expected from solid solution hardening. That obviously means an additional superposition of defect hardening effects leading to high values of the micro-hardness; for 2 at-% Fe:  $HV = 170 \text{ kp/mm}^2$ .

Resistivity measurements, electron microscopy and electron diffraction have been used to investigate the recovery and precipitation behaviour of the alloys. A separate treatment of recovery and precipitation is not possible because the defects are bound to the precipitates.

Resistivity measurements after isochronal annealing show four stages (fig. 1):

I. The first stage reaching from RT to 250 °C can be described by a slightly increasing resistivity for the foil containing 0.5 at-% Fe while the ones with 1 at-% and

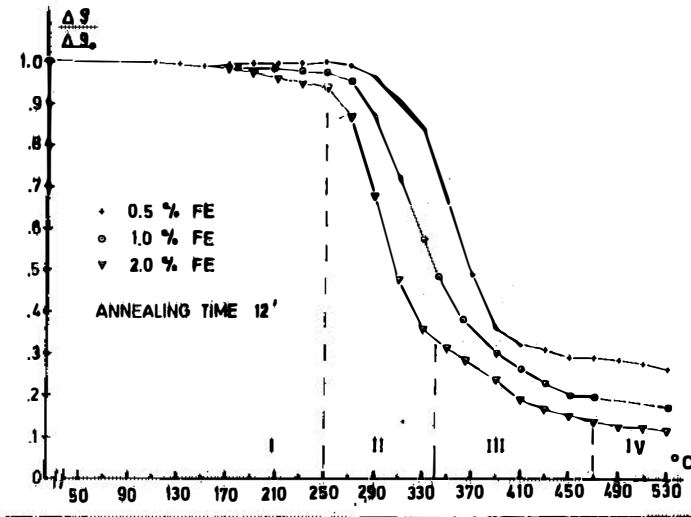


FIG. 1

Resistivity after isochronal annealing;  
annealing time 12 min;  $\Delta T = 20^\circ \text{C}$ .

2 at-% only show a delay of the strong decrease following in the second stage.

- II. The main decrease of resistivity occurs in the second stage. The decrease starts at the same temperature for all investigated foils. The decrease is the more rapid, the higher the concentration of iron.
- III. The beginning of stage III is marked by a change in the slope of the resistivity curves. The degree of recovery and precipitation is the same for all alloys but the temperature at which stage III starts decreases with increasing concentration of iron. This indicates a strong connection between lattice defects and precipitates.
- IV. A further decrease was detected at about  $470^\circ \text{C}$  but could not be investigated more closely because of experimental difficulties.

Electron microscopy and diffraction gave a further insight into the change of the microstructure during the annealing process.

The first stage is marked by coherent and disordered spherical metastable iron-rich particles which can be resolved by

electron transmission using their strain field contrast (fig. 2). The diameter of the zones is estimated to be 30 Å at the end of stage I. The diffraction pattern shows a distortion of the Al matrix, but does not give any evidence for order. The distortion can be seen in the as-quenched state already which suggests the beginning of the decomposition during solidification.

In the second stage the strain field contrast is lost immediately. The crystal structure is very likely a distorted bcc lattice, the structure and orientation relationship of which is being investigated (fig. 3).

At 350 °C the spherical particles are dissolved and formation of rod shaped precipitates begins (fig. 4). These particles are semicoherent and ordered and lie parallel to the <100> directions of the matrix. - Nucleation sites are dislocations or subgrain boundaries. Some of these rod shaped particles continue to grow by bainitic growth mechanism, as indicated by the high frequency of stacking faults, which will have formed by a shear transformation. The same can be seen within particles at grain boundaries (fig. 5). The site at which this bainitic reaction can start requires a complicated defect structure. Therefore not all particles will transform in this way.

Finally incoherent particles are formed during the fourth stage. The structure of these has not yet been determined. It is likely that the equilibrium phases are being formed.

To explain these results we assume that there is a separation into Al-rich regions and Fe-rich zones at the beginning of the annealing process (fig. 6). Starting from the iron concentration of the melt, one has to expect an equilibrium between the  $\theta$  phase  $\text{FeAl}_3$  and an Al-rich solid solution. This equilibrium stage is achieved by a sequence of metastable phases. The assumption is based on:

1. no diffraction effects in addition to those of the Al-

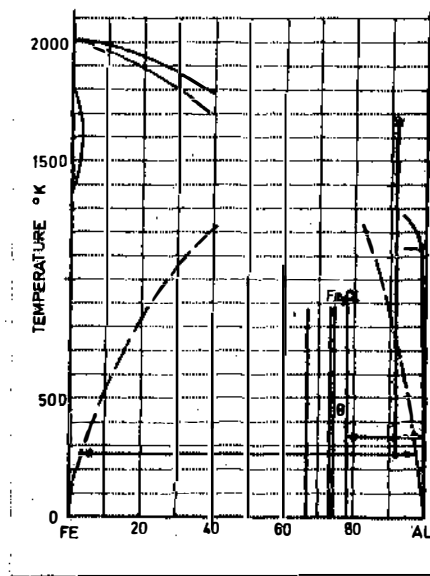


FIG. 6

Phase diagram and tentative shape of the miscibility gap between fcc Al- and bcc Fe-rich solid solution (dotted lines)

- lattice in stage I, indicating presence of a completely coherent phase, and the appearance of additional reflections in stage II (fig. 3);
2. disappearing of strain field contrast is the second evidence for loss of coherency in stage II;
  3. the lattice parameter of the distorted bcc particles is likely to be similar to that of  $\alpha$ -Fe or AlFe;
  4. the more stable phases  $\text{Al}_6\text{Fe}$  and  $\text{Al}_3\text{Fe}$  did not form during the first annealing stages.

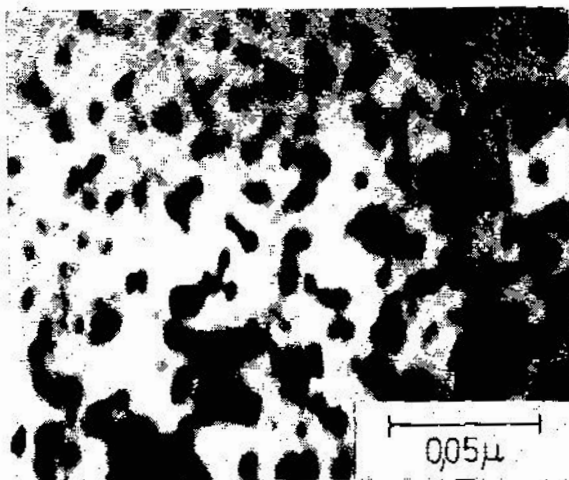


FIG. 2

stage I: Al - 0.5 at% Fe after isochronal annealing for 12 min;  $\Delta T = 20^\circ \text{C}$ ; to  $250^\circ \text{C}$ .

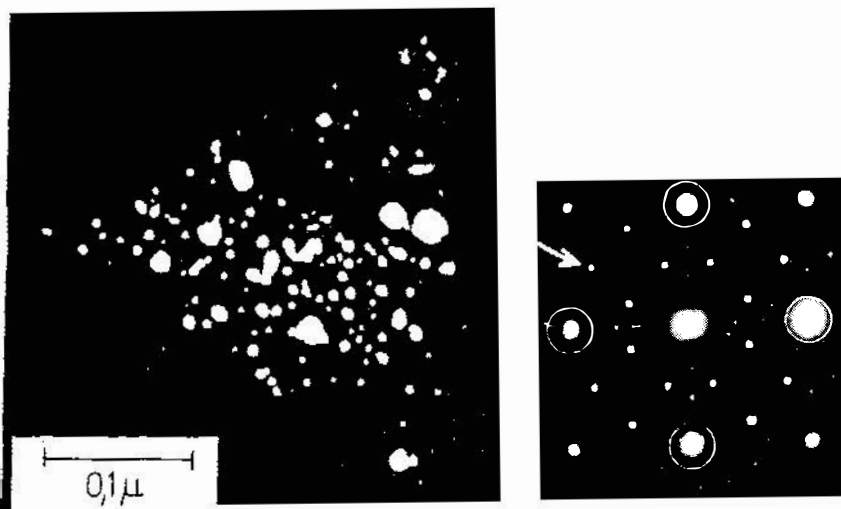


FIG. 3

stage II: Al - 2 at% Fe after isochronal annealing for 12 min;  $\Delta T = 20^\circ \text{C}$ ; to  $370^\circ \text{C}$ . Dark field image made with arrowed reflection.  $\odot$ : reflections from the  $\langle 100 \rangle$  Al matrix which are simultaneously reflections from the precipitates.



A

B

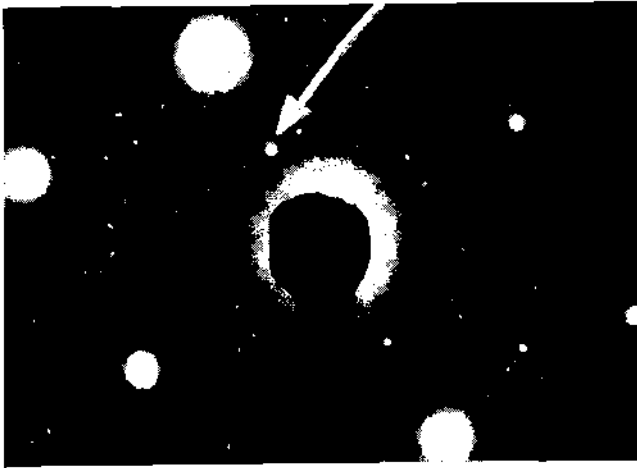


FIG. 4

C

beginning of stage III: Al - 2 at% Fe after isochronal annealing for 12 min;  $\Delta T = 20^\circ\text{C}$ ; to  $410^\circ\text{C}$ . A: bright field. B: dark field showing the rod shaped stage III phase. C: diffraction pattern; the dark field image B is made with the arrowed superlattice reflection.

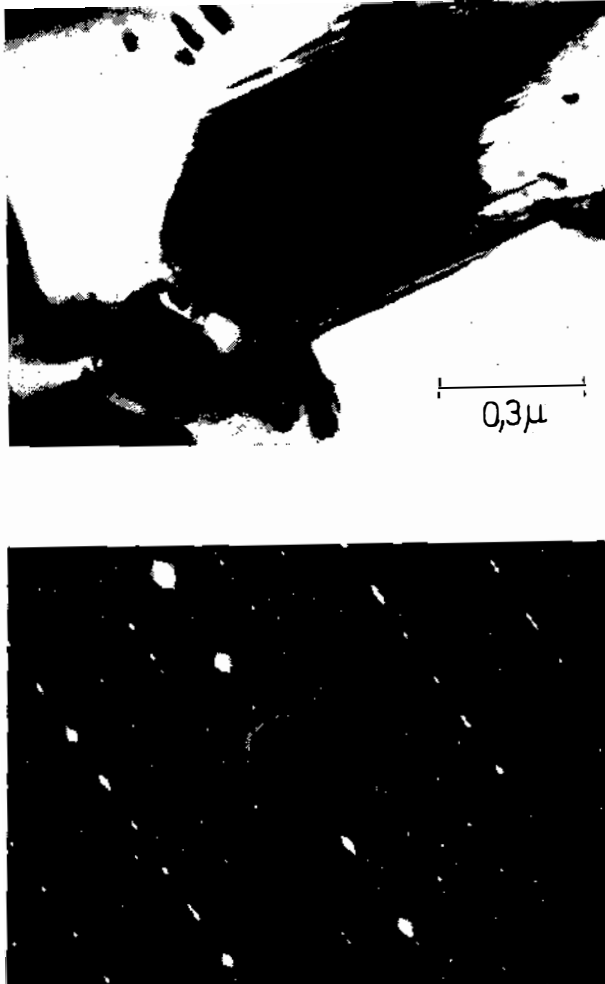


FIG. 5  
Bainitic particles which also occur in stage III .

## DISCUSSION

- R. Roberge : How do you explain the increase in resistivity in the low concentration and the absence of increase in the higher concentration ?
- E. Blank : There is a strong tendency to decomposition increasing with higher concentration of iron. Perhaps the process which causes the increase in resistivity in Al-0.5% Fe happens in the foils with 1% Fe and 2% Fe during solidification.
- A. Guinier : Could you relate your findings about the tetragonal phase with the structures described in the other paper of this session ? Why the zone A and B described by the English team do not appear in the other results ?
- E. Blank : By selected field area diffraction of the dendritic arms I could get also the rings which have been reported by Mr Doggett in his lecture. Bringing some of the globules between the dendritic arms into the selected field area the continuous rings were changed into rings with many single spots. After annealing a solid solution I got a diffraction pattern of the precipitates in stage II which corresponds to the tetragonal structure described just before. The diffraction spots of the precipitates lie on the rings of the dendritic arms. Furthermore the lattice parameters are very similar; ring :  $a = 2.90$ , tetragonal:  $a = 2.86 \pm 0.06$  c/a = 1.10. First, I think the piston and anvil technique has the advantage of cooling the foils from two sides. By an increase of the speed of the piston the foils could be produced thin enough ( $< 10 \mu$ ) to avoid phase separation.
- H. Jones : How can you be sure that your specimens were homogenous ?
- E. Blank : Light microscopy gives a first insight into the existence or non-existence of phase separation, but most information has been obtained by electron microscopy.
- D. Kunstelj : Observations on the Al-1.4 at% Fe (D. Kunstelj and A. Bonefačić, *Metallography*, 2 (1969) 329 ) show that on the scale of applied instrumentation and the specimen preparation technique, the as-obtained samples were homogeneous. Rapid quenching technique used was the "two-piston" method. On annealing at room temperature a precipitation pattern was observed with globular precipitates  $\sim 500 \text{ \AA}$  in dia., along the "cell" - walls inside the grains.

- N.J. Grant : One cannot separate the question of homogeneity for splat cooled foils and the resultant structure because the same doubts must exist regarding all other structures previously reported and now used as reference. To be able to use the term "homogeneous" one must rely on the best analytical tools available to determine this. If these techniques show no second phase, then the term "homogeneous" must apply.
- B. Leontić : High Fe concentrations could be checked by the microprobe. This is a very coarse way. A much better way to do it is by electrical resistivity measurements. One looks at the residual resistivity ratio and observes whether the results agree with the Friedel - Anderson model. If there is any clustering of Fe there will be a deviation.
- P. Furrer : We have examined a great number of Al-Fe alloys prepared by the gun-technique by electron microscopy. (P. Furrer and H. Warlimont, Proc. 7th Intern. Conf. on Electron Microscopy, Grenoble 1970, Vol. 2, p.507). In regions transparent to the electron beam, we could find strongly differing microstructures even within the same foil. A possible explanation is the mode of formation of the splat-cooled foils. The subsequent solidification of small liquid metal globules may result in different cooling rates and various thermal treatments and modes and degrees of mechanical deformation of already solidified material.